# COMPARISON OF X/C-HH INSAR AND L-POLINSAR FOR CANOPY HEIGHT ESTIMATION IN A LODGEPOLE PINE FOREST

**M. Lorraine Tighe[(1)], Doug King[(2)] Heiko Balzter[(3)] and Heather McNairn[(4)]**

[(1)] ***Intermap Technologies*, 200-2 Gurdwara Rd, Ottawa Ontario, K2E 1A2, ltighe@intermap.com**
[(2)] ***Carleton University*, Dept. of Geography and Environmental Studies, 1125 Colonel By Dr. Ottawa, Ontario K1S5B6, Canada, doug_king@carleton.ca**
[(3)] ***University of Leicester*, Department of Geography, Leicester LE1 7RH, UK , hb91@leicester.ac.uk**
[(4)] ***Agriculture and Agri-Food Canada*, 960 Carling Avenue, Ottawa Ontario, K1A 0C6 Canada, mcnairnh@AGR.GC.CA**

## 1. ABSTRACT

Forest canopy height is an important parameter that is strongly correlated with timber volume, biomass, carbon stocks and ecological values such as habitat quality. This parameter is critical to the terrestrial carbon cycle and biomass models and in forest inventory. Remote sensing technologies such as interferometric synthetic aperture radar (InSAR) and polarimetric InSAR (PolInSAR) provide a means to extract canopy height remotely and over large areas. Single-pass X-HH/C-HH InSAR and single-pass L-PolInSAR derived canopy height over Lodgepole pine forest vegetation in Edson, Alberta, Canada are compared to LiDAR derived canopy height. Canopy height of the X-HH and C-HH given by the scattering phase center height ($h_{spc}$) and of the L-PolInSAR given by the Random Volume over Ground (RVoG) DEM difference method indicate an Root Mean Square Error (RMSE) and standard deviation (SD) of 6.84 m ($\pm$3.91 m), 8.20 m ($\pm$6.48 m), and 8.98 m ($\pm$7.66 m), respectively for Lodgepole Pine forest with an average tree height of 28.7 m. A new method to correct for the underestimation of canopy height given by InSAR $h_{spc}$ is presented. To improve the results of the L-PolInSAR DEM difference method, an optimization RVoG 2-D Search phase difference method is presented. These methods obtained an RMSE of 2.15 m ($\pm$2.16 m) and 2.12 m ($\pm$1.93 m) for the X-Band and the L-PolInSAR canopy height models, respectively.

## 2. INTRODUCTION

One of the most vital environmental issues of our time is the sustainable management of the world's forest resources. Furthermore, the demand for forest products is increasing while forested area continues to diminish [1]. Forest canopy height is a key parameter in forest inventory and ecological process modeling. It is strongly correlated to timber volume and biomass, and is critical in modeling of the terrestrial carbon cycle, fire prediction, and species habitat. However, manual field measurement of tree height using conventional techniques is time-consuming, costly, and restricted to selected sample locations. The ability to derive forest canopy height over spatially extensive areas would therefore be of great benefit. Considerable advances in remote sensing technologies have led to a new era of global topographic observations, where reliable forest measurements are becoming a possibility [2] [3]. Two of the most promising technologies are interferometric synthetic aperture radar (SAR) known as InSAR [4] [5] [8] and polarmetric InSAR (PolInSAR) [6] [7] [9] [10]. Phased-based InSAR techniques exploit the interference patterns of two electromagnetic waves to remove the random component of phase of the single complex radar signal in order to estimate the first surface feature height given by the scattering phase center height ($h_{spc}$). The $h_{spc}$ of a forested canopy may include elevations of the tree top, tree leaves, twigs and branches, tree trunks, undergrowth, the edge of a tree canopy, and/or a ground contribution [10 [11] [12] [13 [14] [8]. Where the $h_{spc}$ generally lies within a forest canopy and the subsequently derived digital surface model (DSM) is dependent on the system parameters (wavelength, SAR polarization, and incidence angle), terrain characteristics (vegetation type, structure and density, slope, soil and vegetation moisture) and DSM processing techniques (e.g., elevation posting, fusion of multiple data takes) [14] [15] [16] [17] [18]. X- and C-Band InSAR, for example, typically measure elevations from the upper part of the canopy with little signal penetration to the ground. At longer wavelengths (L-/P-Band), attenuation is lower but can still be significant [19]. Success in the estimation of canopy height has been reported using several InSAR methods such as $h_{spc}$ (the subtraction of an InSAR derived DSM from a reliable DTM) [8] [12] [13] [22] [24], height discontinuity (relies on the boundary between a tree canopy and an adjacent cleared area to derive the $h_{spc}$) [20] [21], and dual frequency method (e.g. the subtraction of the ground surface given by low frequency L- or P-band InSAR from high frequency X- or C-band data to yield $h_{spc}$) [13] [25]. A recent technique to derive bare ground and canopy height measurements combines polarimetry and interferometry, referred to as PolInSAR, first introduced

*Proc. of '4th Int. Workshop on Science and Applications of SAR Polarimetry and Polarimetric Interferometry – PolInSAR 2009', 26–30 January 2009, Frascati, Italy (ESA SP-668, April 2009)*

by Cloude and Papathanassiou [26] [27]. PolInSAR techniques are based on the coherent combination of the prevalent scattering mechanisms (SAR polarimetry) and the vertical location of scatterers (SAR interferometry) which are substantially more sensitive to forest structural parameters than conventional interferometry or polarimetry alone [28] [29] [30]. Combining polarimetric and interferometric data therefore results in information about the penetration depth into the canopy at different polarizations [30]. One parameter that limits the performance of PolInSAR inversion is repeat-pass data collection where temporal decorrelation (affects derived tree height accuracy). This paper utilizes data from the world's first single-pass L-PolInSAR system, resulting in higher coherence, less volume decorrelation and no temporal decorrelation over vegetated areas in comparison to repeat-pass PolInSAR. Data from single-pass X- and C-Band InSAR data are compared to the L-Band PolInSAR data and to LiDAR canopy height data to investigate the use of InSAR/PolInSAR data for operational forestry applications.

### 2.1 Research objectives

A significant amount of research has been published on InSAR and PolInSAR for forest parameters; however, research is still needed to gain further understanding of how SAR signals interact with forests and how this interaction can be exploited for operational use in forestry applications. This study compares InSAR/PolInSAR derived canopy height over dense homogenous Lodgepole pine (*Pinus contorta*) to LiDAR derived canopy height. The objectives were to first, compare canopy height retrieval based on X- and C-HH-polarized InSAR $h_{spc}$ and L-band PolInSAR RVoG inversion phase difference with a LiDAR derived canopy height model (CHM). Second, to test a new method that corrects for the underestimation of the canopy height given by InSAR $h_{spc}$. Third, to test an optimized L-Band PolInSAR tree height retrieval algorithm, based on the RVoG inversion 2-D Search technique put forth by [39].

## 3. STUDY SITE AND DATA

### 3.1 Study Site

The study area is located near Edson, Alberta, Canada, approximately 200 km west of Edmonton. It was chosen to represent dense homogenous coniferous forests with little understory in a temperate continental environment. Geographically the site covers an 849 $m^2$ and is located approximately between 53°11'16.90" N and 53°11'58.06" N latitude and 116°43'38.30"W and 116°44'15.58"W longitude (Figure 1, red dot). The site consists of three dense forested patches surrounded by grass or barren fields. The forested areas are comprised of Lodgepole pine trees with an average tree height of 28.7 m. The terrain is flat (elevation range of 1,090 to 1,121 m (Δ31 m)).

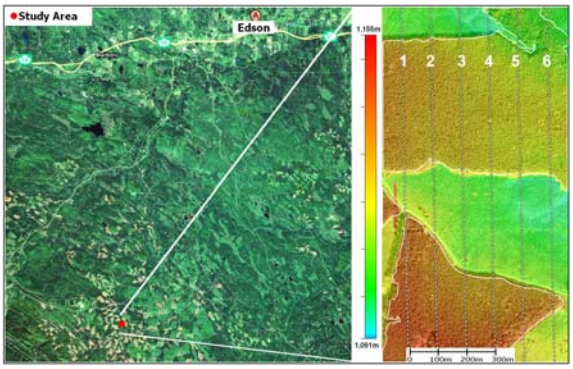


*Figure 1. Study site location on Google Earth image (left image); six transect lines superimposed on fused aerial imagery and LiDAR elevation data (right image).*

### 3.2 INSAR DATA

Single-pass airborne X-HH and spaceborne C-HH InSAR data and single-pass airborne L-Band PolInSAR data are utilized herein. Each dataset is described in detail in the following sections (Table 1, Figure 2).

*Table 1. InSAR datasets available for the study site.*

| Data | System | Elevation Products | Collection Date |
|---|---|---|---|
| X-HH InSAR | Intermap STAR | DSM, 2 m GSD, 1 m (Vertical) and 2 m (Horizontal) RMSE Accuracy | 3-Apr-06 |
| C-HH InSAR | SRTM | DSM, 90m GSD, 16m RMSE Vertical Accuracy, 16m Horizontal Accuracy | 11-Feb-00 |
| L-HH PolInSAR | Intermap TopoSAR-L | DSM & DTM, 2 m GSD, TBD m (Vertical) and 2 m (Horizontal) RMSE Accuracy | 24-Jun-08 |

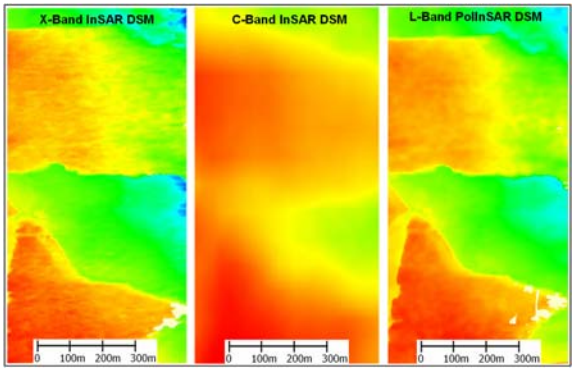


*Figure 2. Surface elevation model (DSM) data, from left to right: X-HH InSAR, C-HH InSAR, and. L-Band PolInSAR*

#### 3.2.1 Single Pass Airborne X-HH InSAR Data

Intermap Technologies Inc. (Intermap, 2008) commercially operates several airborne single-pass X-Band InSAR sensors. These sensors, called STAR technologies, are high-resolution across-track InSAR mounted in airborne platforms (e.g. King Air, Lear Jet 36) [34]. STAR3 was used to collect the X-HH data.

Details of this sensor are provided in Table 2 [7]. The X-HH InSAR data were single pass (no fusion from other passes) and interferometrically processed by Intermap using a proprietary IFPROC processor, previously described in [32] [33]. The X-HH data represent a first surface model called a digital surface model (DSM) with a 2 m ground sampling distance (GSD) processed to a 32 bit floating grid. Corresponding orthorectified radar imagery (ORI) has a 2 m pixel was processed to an 8 bit geotiff.

*Table 2. Intermap STAR3 Platform Specifications.*

| SENSOR | STAR3 |
|---|---|
| Platform | Learjet 36A |
| Flying Height/Speed | 10,000 m 700 km/hr |
| Wavelength | 3 cm X-Band |
| Frequency | 9.6 GHz |
| Polarization | HH |
| Interferometric Baseline | 1 m |
| Depression Angle | Centered on 45°; Range 35°-55° |
| DSM/DTM Posting | 2m |
| ORI Pixel Size | 2m |
| Horizontal Accuracy | 2m |
| Vertical Accuracy | 1m |

### 3.2.2 Single Pass Spaceborne C-HH InSAR Data

The Shuttle Radar Topography Mission (SRTM) was flown on board the Space Shuttle Endeavour during mission STS-99 February 11-22, 2000 (Table 3). Additional details of the SRTM data are found in [6] [12] [17] [35]. 99.97% of the targeted land mass was mapped with at least one data pass (i.e., one Shuttle overpass), 94.59% with at least two data passes, 49.25% with at least three data passes, and 24.10% with at least four data takes. The quality of the SRTM data may suffer from mast motion and phase noise errors [7]. SRTM data were obtained for the study site at an Interferometric Terrain Height Data 1 (ITHD-1) specifications which include 90 m spatial sampling, 30 m absolute vertical height accuracy, and 20 m absolute horizontal accuracy and at the same mapping projection (WGS84) as the X-/L-band data sets. All accuracies are quoted at the 90% confidence level [34].

*Table 3. SRTM Platform Specifications.*

| SENSOR | SRTM |
|---|---|
| Platform | Space Shuttle STS-99 |
| Flying Height/Speed | 233 km |
| Wavelength | 5.8 cm C-Band |
| Frequency | 5.3 GHz |
| Polarization | HH |
| Interferometric Baseline | 60 m |
| Depression Angle | 57° |
| DSM/DTM Posting | 90 m |
| Horizontal Accuracy | 30 m |
| Vertical Accuracy | 16 m |

### 3.2.3 Single Pass Airborne L-PolInSAR Data

In 2007, Intermap Technologies developed the world's first airborne single-pass, cross-track, fully polarimetric, interferometric radar sensor operating in L-Band (22 cm, 1.325 GHz) to create bare-earth digital elevation models (DEMs or DTMs) and to determine forest canopy height [31]. This system, called TopoSAR-L, is an adaptation of the TopoSAR System [4]. Table 4 provides a list of the specifications of the TopoSAR-L system. Additional details are given in [31]. TopoSAR-L's geometric baseline, in combination with the operating flight altitude of 1000m, allows for the derivation of ORI, DSM and DTM products with a 2 m GSD. The TopoSAR-L DSM and DTM were processed as 32-bit floating grids and the ORI was processed as an 8-bit image.

*Table 4. Intermap TopoSAR-L Platform Specifications.*

| SENSOR | TopoSAR-L |
|---|---|
| Platform | Gulfstream Twin Commander 695 N808NC |
| Flying Height/Speed | 1000 m |
| Wavelength | 22 cm L-Band |
| Frequency | 1.26 - 1.39 GHz |
| Polarization | HH, VV, HV, VH |
| Interferometric Baseline | 3.5 m (ping-pong) |
| Depression Angle | 35° - 55° |
| DSM/DTM Posting | 2 m |
| Horizontal Accuracy | Expected 5 m |
| Vertical Accuracy | Expected 5 m |

## 3.3 ANCILLARY DATA

High resolution (0.4m pixels) color aerial photography (September 2007) was acquired from Valtus Aerial Photography. The Lodgepole pine vegetation boundaries were digitized from the air photo (Figure 1). LiDAR derived bare ground data (used as the reference DTM) and full featured point cloud (used to extract the reference DSM) was available for validation of the canopy height models. The LiDAR data were collected by Terrapoint's Mid-Range LiDAR system. It is a 2D laser scanner that produces 8-20 points per square meter coverage even in densely vegetated areas. The LiDAR data have a stated vertical accuracy (95% confidence level) of 0.10-0.30m on vegetated surfaces over flat to rolling terrain (which is the case for this study site). The horizontal accuracy (95% confidence level) is 0.15-0.75m in all but extreme hilly areas. The bare ground data (referred to as a DTM) were provided as a 2 m GSD 32-bit floating grid. A DSM was derived from the LiDAR point cloud by taking the highest point within a 5.6 m search radius based on the provided 1 m GSD point cloud. The resultant LiDAR DSM grid was resampled to a 2 m GSD 32-bit floating grid to correspond with the other elevation data sets.

## 4. METHODS

### 4.1 Transect Lines

Six transect lines (Figure 1) were established running north-south through the study area. Transects were

spaced 100 m apart with sample points spaced 10 m apart along each transect line. The height at each sample point was extracted from the LiDAR canopy height model (CHM; section 4.2) and the LiDAR DSM and used as the reference data. The height at each sample point was also derived for the $h_{spc,}$ X- and C-Band surfaces (section 4.3), the L-Band phased difference height surface (4.3), the PolInSAR (4.4 - 4.5) and the X-band derived (CHMs) (4.5) for comparison with the LiDAR reference data.

### 4.2 LiDAR Canopy Height Model – Reference Data

The LiDAR bare ground data were subtracted from the LiDAR derived DSM data to generate a canopy height model (CHM) of the study site (Figure 3). The LiDAR CHM was used as the reference CHM.

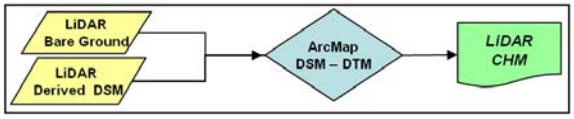


*Figure 3. Methodology to derive LiDAR canopy height model.*

### 4.3 Scattering Phase Center Estimation

The $h_{spc}$ was directly estimated from X- and C-Band phased InSAR by subtracting the LiDAR DTM from an InSAR DSM data (Figure 4) [12] [24]. This approach was applicable because the as the X- and C-Band InSAR sensors operate at a short wavelength so that the majority of the scattering comes from the upper portion of the vegetation canopy. The LiDAR provided a reliable bare ground elevation model in support of this approach.

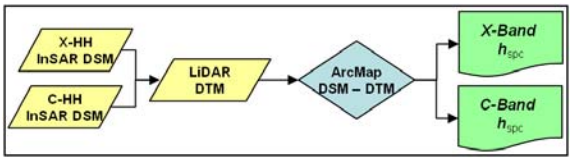


*Figure 4. Methodology to calculate scattering phase center height for InSAR data.*

### 4.4 PolInSAR Canopy Height and Bare Ground Estimation

The application of PolInSAR is for estimating canopy height is not straightforward because of the complex structure of forests; it requires the consideration of a scattering model. The Random Volume over Ground (RVoG) model has been frequently utilized [6] [10] [29] [39]. RVoG assumes vegetation to be a conglomerate of randomly oriented scatterers situated above a surface layer (bare ground) [10] [40]. The interferometric phase related to ground topography and canopy height can be extracted according to the RVoG model by a simple mathematical extrapolation process [6] [10] [29] [39].

The complex interferometric coherence $\tilde{\gamma}$ can be written equation (1) [10].

$$\tilde{\gamma}(\vec{w}) = \exp(i\phi_0)\frac{\tilde{\gamma} + m(\vec{w})}{1 + m(\vec{w})} \qquad (1)$$

Where $\phi_0$ is the ground topography phase, m is the effective ground-to-volume amplitude ratio (which accounts for attenuation though volume) and $\vec{w}$ represents the polarization state. $\tilde{\gamma}_v$ Is the complex coherence for the volume (excludes ground component), and $\sigma$ is a function of the extinction coefficient for the random volume thickness is given by $h_v$ in equation (3).

$$\tilde{\gamma}_v = \frac{\int_0^{hv} \exp(ik_z z')\exp\frac{2\sigma z'}{\cos\theta_0})dz'}{\int_0^{hv} \exp(\frac{2\sigma z'}{\cos\theta_0})dz'} \qquad (3)$$

Where $k_z$ is the vertical number calculated from the incidence angle ($\theta$), the difference in the two incidence angles ($\Delta\theta$), and the wavelength ($\lambda$) of the radar system as in Equation (4).

$$K_z = \frac{4\pi\Delta\theta}{\lambda \sin\theta} \quad \text{Radians/meter} \qquad (4)$$

Here we make the assumption that $\tilde{\gamma}_v$ is not polarization dependent while m is. A coherence optimization process is then used to identify optimum coherence values that will lie upon a straight line (red crosses, Figure 5) as a function of m within the unit circle (yellow ellipsoid, Figure 5) on the complex plane by manipulating Equation (1) [40]. The intersection of this line with the unit circle provides the topographic phase (navy circle, Figure 5) for large m and the associated phase at this point relates directly to the ground elevation.

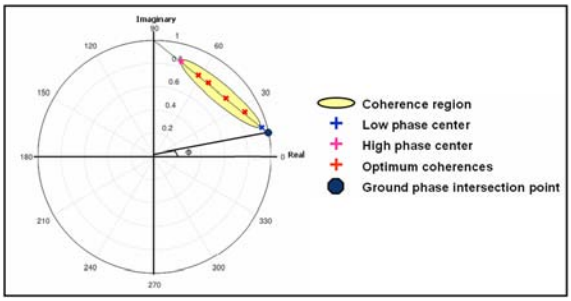


*Figure 5. PolInSAR ground topography and canopy height extraction in the complex plane, for one image pixel. The ellipse-shaped region (yellow) denotes the area in which all possible coherences lie.*

A limit of no ground component (m=0), the observed coherence is given by the volume coherence $\vec{\gamma}_v$ rotated through $\phi_0$. To obtain canopy height, much of the effort in PolInSAR has been to develop robust methods to estimate $h_V$ through an inversion process [6] [9] [39] [40]. Two methods are presented here, the DEM difference and the 2-D Search were applied to L-Band 10m baseline dataset.

#### 4.4.1 PolInSAR DEM Difference Method

In the DEM differencing method, the forest height hv is estimated directly from the phase difference between ground phase and the volume-dominated polarization phase [27]. While this method is a simple implementation of RVoG and computationally light, it tends to underestimate canopy height because the interferometric phase centre is seldom near the top of the canopy.

#### 4.4.2 PolInSAR 2-D Search Method

In the 2-D Search method, a look-up table (LUT) containing values of random volume interferomteric coherences as calculated in Equation (1) is established, using a set of extinction coefficient values and forest height values and displayed in the complex plane [40]. Estimated complex interferometric coherence according to Equation (1) assuming no ground return (m=0) with σ=0, 0.1,…,1.0db/m from centre to outer and hv=0-40m with 0.5m as step. A search to find closest element in the LUT to the observed complex coherence, we can estimate extinction coefficient and forest height at the same time [9]. The high phase end is used in the height inversion. While the 2-D search with a fine LUT (small step size for hv and σ) achieved increased canopy height accuracy, it does so at the cost of increased computation time. Knowledge of the forest height and mean extinction coefficient can guide the search and reduce computation time.

### 4.5 Phase Difference Height Estimation

The L-Band PolInSAR DSM represents a combination of scatters at HH, VV, HV, and VH polarizations and thus do not reflect a scattering phase center height in the same manner as with the single polarized X- and C-Band InSAR data. The subtraction of an accurate DTM from the L-PolInSAR derived DSM is instead, referred to as phase difference height. Three phase difference height calculations were performed using the L-PolInSAR data (Figure 6). First, the L-PolInSAR (L-PolInSAR1) DTM created from the DEM difference method was subtracted from the L-PolInSAR DSM to derive the first phase difference, namely L1-PolInSAR. Second, the LiDAR DTM was subtracted from the L-PolInSAR1 DSM to derive L2-PolInSAR phase difference. Third, the LiDAR DTM was subtracted from the 2-D search derived L-PolInSAR (PolInSAR2) DSM to obtain the L3-PolInSAR phase difference. Figure 6 provides an illustration of the process flow utilized to create all three L-PolInSAR phase differences.

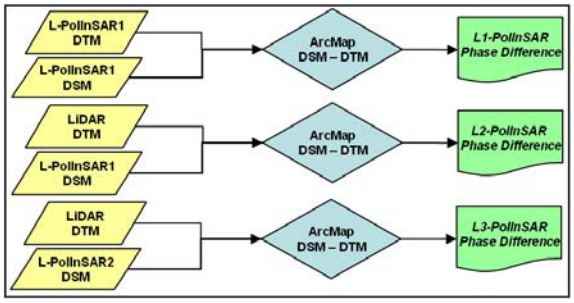


*Figure 6. Three L-Band phase height difference calculations.*

### 4.6 InSAR Canopy Height Model (CHM)

A new method to account for the attenuation of the microwave radiation into the canopy at short wavelengths (e.g. X- and C-band) is proposed for InSAR data (Figure 7). This method utilizes the percentage of tree height underestimation caused by penetration of microwave radiation into the canopy (equation (4)), the type of vegetation canopy (e.g. given by land cover derived from the aerial photography) and the scattering phase center height ($h_{spc}$) derived from the InSAR DSM and an accurate DTM. This method was applied to the X-HH InSAR data to derive a refined CHM from X-Band InSAR data (Figure 7). It was not applied to the C-Band InSAR data as it was through to be suspect.

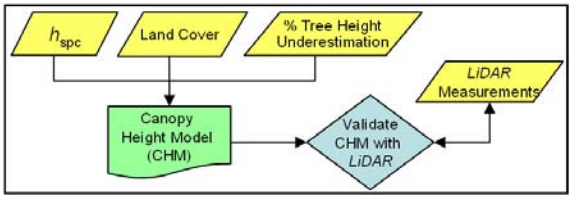


*Figure 7. Flowchart that illustrates the components of the proposed Canopy Height Model (CHM).*

## 5. RESULTS AND DISCUSSION

### 5.1 PolInSAR Bare Ground Analysis

The DEM difference RVoG method was used to derive a DTM from the L-Band PolInSAR data for the study site. The DTM performed well over barren land cover; however, improvements beneath the vegetation are required. Figure 8 demonstrates both over and underestimation of the terrain height by the PolInSAR RVoG DEM difference derived DTM relative to the

LiDAR DTM. The L-Band DTM achieved an accuracy of 5.31 m RMSE (5.49m, CE95) through dense forest canopy when compared to the LiDAR DTM. Similar results were found in [31].

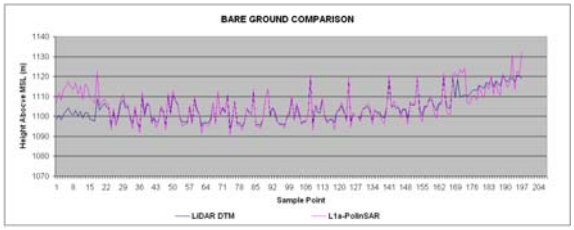


*Figure 8: LiDAR DTM (navy) and L1a-PolInSAR DTM (pink) for the transect lines 1-3.*

### 5.2 Scattering Phase Center and Phase Difference Height Analysis

Retrieved heights from sample points along the six transect lines (Figure 1) were extracted from the X- and C-Band $h_{spc}$ and L-PolInSAR phase differenced height surfaces and compared with the LiDAR CHM by calculating the Root Mean Square Error (RMSE), standard deviation (SD), 95% circular error confidence level (CE95) and the percentage of canopy height underestimation caused by penetration of microwave radiation into the canopy given by equation (4). Results are tabulated in Table 5.

$$E(h_{canopy}) = \left(1 - \left(h_{spc} - h_{LiDAR}\right)\right) * 100 \qquad (4)$$

Where $h_{spc}$ is the InSAR scattering phase center height or PolInSAR phased difference height and $h_{LiDAR}$ is the reference CHM. Table 5 indicates noticeable discrepancies/limitations between the X-HH/C-HH InSAR $h_{spc}$ and L-PolInSAR phase difference results compared to the LIDAR CHM. As expected, the $h_{spc}$ models underestimate canopy height at X-Band wavelength [13] [14] [15] [24] because it does not account for the downward penetration of the SAR signal (attenuation) into the canopy, which, at shorter wavelengths underestimates the forest canopy by 29.09% (X-HH) for Lodgepole pine trees with an average tree height of 28.7 m for this study site.

*Table 5. Scattering phase center height and phase difference height error assessment (average tree height 28.7 m).*

| Average Tree Height is 28.7 m* Wavelength | RMSE (m) | SD | CE95 | Tree Height Underestimation* |
|---|---|---|---|---|
| X-Band $h_{spc}$ | 8.35 | ±1.83 | 11.61 | 29.09% |
| C-Band $h_{spc}$ | 4.44 | ±4.42 | 7.78 | -15.47% |
| L2 PolInSAR DSM - LiDAR DTM | 8.29 | ±2.06 | 10.92 | 28.89% |
| L1 PolInSAR DSM - PolInSAR DTM | 13.81 | ±2.98 | 17.76 | 48.12% |

The C-Band $h_{spc}$ model which over- and under-estimates the canopy height by -15.47%. Others have found similar results [8] [17] [18]. The LiDAR CHM, X-HH/C-HH Band $h_{spc}$ and the two L-PolInSAR phase difference models for transect lines 1 and 2 are depicted in Figures 9 and 10, respectively. The X-Band $h_{spc}$ and L-PolinSAR (L2) phase difference canopy height are similar and slightly lower than the LiDAR canopy height model. The C-band overestimates the canopy height by 15.47%.

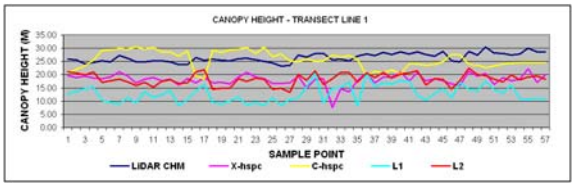


*Figure 9: LiDAR CHM (navy), X-$h_{spc}$ (pink), C-$h_{spc}$ (yellow), and PolInSAR phase difference models L1 (turquoise) and L2 (red) phase difference models for transect line 1 (average tree height = 28.7 m).*

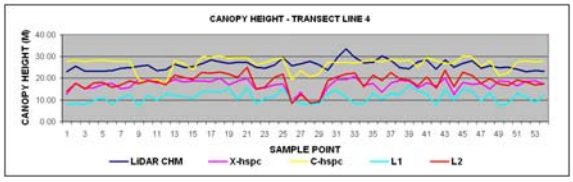


*Figure 9: LiDAR CHM (navy), X-$h_{spc}$ (pink), C-$h_{spc}$ (yellow), and PolInSAR phase difference models L1 (turquoise) and L2 (red) phase difference models for transect line 2 (average tree height = 28.7 m).*

### 5.3 Canopy Height Model Optimization

The C-Band data were thought to be suspect. Reference [7] indicates that error mitigation strategies to compensate for phase noise and motion mast errors are recommended when using SRTM data to retrieve canopy height. Due to time constraints, such mitigation strategies were not performed in this study, thus the CHM was not applied to the C-Band data.

Retrieved heights from sample points from the Lodgepole pine forests along transect lines (Figure 1) for the X-Band CHM (described in 4.6) and the L3 (L-PolInSAR 2-D Search phase difference DSM – LiDAR DTM, section 4.5) CHM were compared with the LiDAR CHM by calculating the RMSE, SD, CE95, and the percentage of canopy height underestimation given by equation (1). To reduce forest edge effects, samples located up to 6 m (3 pixels) from the forest cover boundaries were excluded. The results are presented in Table 6 and Figure 11. An RMSE of 2.15 m (±2.16 m) and 2.12 m (±1.93 m) were obtained for the X-Band and the L-PolInSAR optimized CHMs, respectively.

*Table 6. Canopy height model comparison.*

| Canopy Height Model (CHM) Error Assessment Against LiDAR CHM | | | | |
|---|---|---|---|---|
| Wavelength | RMSE (m) | SD | CE95 | Tree Height Underestimation* |
| X-Band CHM | 2.15 | ±2.16 | 4.14 | 7.49% |
| L-PolInSAR2 Phase Diff. | 2.12 | ±1.93 | 3.68 | 7.39% |
| Average Tree Height is 28.7 m* | | | | |

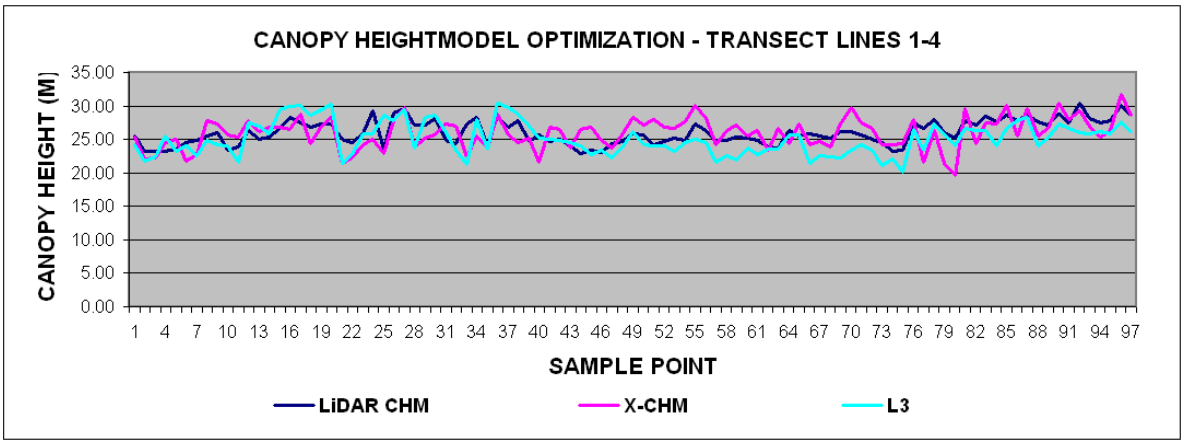


*Figure 11: Canopy height over forest stands (average height = 28.7 m) for LiDAR-CHM (navy), X-CHM (pink), and L3-PolInSAR phase difference (turquoise).*

## 6. CONCLUSIONS

In this study we have shown that the X-HH $h_{spc}$ compared to the LiDAR canopy height indicated that the scattering phase center of X-Band InSAR is located clearly below the forest canopy. Results indicate that the SRTM C-Band InSAR $h_{spc}$ overall overestimated the canopy height, which was unexpected. The C-Band data is considered to be suspect and thus warrants further investigation. The L-Band PolInSAR RVoG techniques were used to extract the bare ground and canopy elevations. Additional testing of the L-Band PolInSAR DEM difference method is required to better separate the volume and ground scattering to achieve better DTM results beneath forest canopy. We have demonstrated that canopy height estimation by means of a new canopy height model for X-band InSAR and by means of L-PolInSAR inversion of the RVoG 2-D Search model works well for homogeneous Lodgepole Pine forests with an average height of 28.7 m for this region. Both models agree well with the LiDAR derived CHM; however, they rely on an accurate DTM model. Field measurements of tree height and bare ground elevations would provide validation of the LiDAR data and the CHM. X-band InSAR and PolInSAR canopy height methods need to be tested on other terrain and vegetation types to determine their applicability.

## 7. ACKNOWLEDGEMENTS

The authors would like to thank Dr. Q. Zhang and Dr. B. Mercer at Intermap for the processing of the L-PolInSAR and LiDAR data. A special thanks to K. Chaney for the editing of this document.

## 8. REFERENCES

[1] Gullison, R., Frumhoff, P., Canadell, F., Field, C., Nepstad, D., Hayhoe, K., Avissar, R., Curran, L., Friedlingstein, P., Jones, C. & Nobre C. (2007). Tropical Forests and Climate Policy. *Science* **316**(18), 985-986.

[2] Homer, C., Dewitz, J., Fry, J., Coan, M., Hossain, N., Larson, C., Herold, N., McKerrow, A., VanDriel, J. & Wickham, J. (2007). Completion of the 2001 National Land Cover Database for the conterminous United States. *Photogrammetric Engineering and Remote Sensing*, **73**(4), 337–341.

[3] Maune, D.F. (2007). Digital Elevation model Technologies and Applications: *The DEM Users Manual, 2nd Edition, ASPRS*.

[4] Madsen, S.N., Zebker, H.A. & Martin, J. (1993). Topographic mapping using radar interferometry: processing techniques, *IEEE Transactions on Geoscience and Remote Sensing*, **31**, 246-256.

[5] Hensley. S., Munjy R. &. Rosen, P. (2001). Interferometric synthetic aperture radar (IFSAR), digital elevation model technologies and applications: *The DEM users' manual, ASPRS*, Chapter 6, 174-176.

[6] Cloude, S. & D. Corr. (2003). Tree height retrieval using single baseline polarimetric interferometry. *Polinsar ESA Workshop, Frascati, Italy*.

[7] Mercer, B. (2004). DEMs created from airborne IFSAR an update, *International Archives of Photogrammetry and Remote Sensing*. **35(**B), CD-ROM.

[8] Walker, W., Kellndorfer, J. & Pierce, L. (2007). Quality assessment of SRTM C- and X-band interferometric data: Implications for the retrieval of vegetation canopy height. *Remote Sensing of Environment*, **106**, 428–448.

[9] Zhang, Q., Mercer, B. & Cloude, S. R. (2008). Forest height estimation from INDREX-II L-band polarimetric InSAR data. *The International Archives of the Photogrammetry, Remote Sensing and Spatial Information Science,* **XXXVII**(Part B1), 343-348.

[10] Treuhaft R. & Siqueira, P. (2000). Vertical structure of vegetated land surfaces from interferometric and polarimetric radar. *Radio Science*, **35**(1), 141–177.

[11] Hodgson, M., Jensen, J., Tullis, J., Riordan, K. & Archer, C. (2003). Synergistic use of LiDAR and color aerial photography for mapping urban parcel imperviousness. *Photogrammetric Engineering and Remote Sensing*, **69**(9), 973–980.

[12] Kellndorfer, J., Walker, J., Pierce, L., Dobson, C., Fites, J. & Hunsaker, C. (2004). Vegetation height estimation from shuttle radar topography mission and national elevation datasets. *Remote Sensing of Environment*, **93**, 339−358.

[13] Balzter, H., Luckman, A., Skinner, L., Rowland, C. & Dawson, T. (2007): Observations of forest stand top height and mean height from interferometric SAR and LIDAR over a conifer plantation at Thetford Forest, UK. *International Journal of Remote Sensing*, **28(**6), 1173 - 1197.

[14] Andersen, H., Mcgaughey R. & Reutebuch, S. (2008). Assessing the influence of flight parameters, interferometric processing, slope and canopy density on the accuracy of X-band IFSAR-derived forest canopy height models. *International Journal of Remote Sensing*, **29**(5), 1495-1510.

[15] Izzawati, E., Wallington, D. & Woodhouse, I. (2006). Forest height retrieval from commercial X-band SAR products. *IEEE Transactions on Geoscience and Remote Sensing*, **44**, 863–870.

[16] Dall, J. 2007. InSAR elevation bias caused by penetration into uniform volumes. *IEEE Transactions on Geoscience and Remote Sensing*, **45**(7), 2319-2324.

[17] Beck, K. (2008). Investigation of elevation bias of the SRTM C- and X-Band Digital elevation Models. *International Archives of the Photogrammetry, Remote Sensing and Spatial Information Sciences*, **XXXVII**(Part B1), 105-110.

[18] Viergever, K., Woodhouse, I., Marino, A., Brolley M. & Stuart, N. (2008). Sar interferometry for estimating above-ground biomass of savannah woodlands in Belize. *IEEE Transactions on Geoscience and Remote Sensing*, in press.

[19] Bessette, L. & Ayasli, A. (2001). Ultra-wideband P-3 and CARABAS II foliage attenuation and backscatter analysis. *Proceedings of the 2001 IEEE Radar Conference, Atlanta, GA, USA*, 357-362.

[20] Hagberg, J., Ulander, M. & Askne, J. (1995). Repeat-pass SAR interferometry over forest terrain. *IEEE Transactions on Geoscience and Remote Sensing*, **22**(2), 331-340.

[21] Woodhouse, I., Izzawati, Wallington, I. & Turner, D. *(*2006). Edge Effects on Tree Height Retrieval Using X-Band Interferometry. *IEEE Geoscience and Remote Sensing Letters*, **3**(3), 344-348.

[22] Kobayashi, Y., Sarabandi, K., Pierce, L. & Dobson, C. (2000). An evaluation of the JPL TOPSAR for extracting tree heights. *IEEE Transactions on Geoscience and Remote Sensing*, **38**, 2446−2453.

[23] Brown, C. & Sarabandi, K. (2003). Estimation of red pine tree height using shuttle radar topography mission and ancillary data. *IGARSS, Toulouse*, 2850–2852.

[24] Balzter, H., Rowland, C. S. & Saichc, P. (2007). Forest canopy height and carbon estimation at Monks Wood National Nature Reserve, UK, using dual-wavelength SAR interferometry, *Remote Sensing of Environment*, **108**(3), 224-239.

[25] Andersen, H., McGaughey, R., Reutebuch, S., Schreuder, G., Agee, J. & Mercer, B. (2004). Estimating canopy fuel parameters in a Pacific Northwest conifer forest using multifrequency polarimetric IFSAR. I*nternational Archives of Photogrammetry and Remote Sensing, Istanbul, Turkey*, **XXXV**(Part B).

[26] Cloude, S. & Papathanassiou, K. (1997). Polarimetric optimization in radar interferometry. *Electronic Letters*, **33**(13), 1176–1178.

[27] Cloude, S. & Papathanassiou, K. (1998). Polarimetric SAR interferometry. *IEEE Transactions on Geoscience and Remote Sensing*, **36**(5), 1551-1565.

[28] Treuhaft, R., Madsen, S., Moghaddam, M. & van Zyl, J. (1996). Vegetation Characteristics and Underlying Topography from Interferometric Data**.** *Radio Science*, **31**, 1449-1495.

[29] Papathanassiou, K. & Cloude, K. (2001). Single-baseline polarimetric SAR interferometry. *IEEE Transactions on Geoscience and Remote Sensing*, **39**(11), 2352−2363.

[30] Rowland, C., Balzter, H., Cox, R., Saich, P. & Stebler, O. (2003). The CORSAR project: can polarimetric SAR interferometry improve forest biomass estimation. *POLINSAR 2007*.

[31] Mercer, B. & Zhang, Q. (2008). Recent advances in airborne InSAR for 3D Applications. *International Archives of the Photogrammetry, Remote Sensing and Spatial Information Sciences*, **XXXVII**(Part B1), 141-146.

[32] Tighe, M. L., 2000. Topographic Line Map Production Using High Resolution Airborne Interferometric SAR. *IAPRS*, **XXXIII**, Amsterdam.

[33] Intermap Product Handbook, 2008. Link: http://www.intermap.com/interior.php/pid/3/sid/311.

[34] Rabus, B., Eineder, M., Roth, A. & Bamler, R. (2003). The shuttle radar topography mission—a new class of digital elevation models acquired by spaceborne radar. *ISPRS Journal of Photogrammetry and Remote Sensing*, **57**(4), 241-260.

[35] Hensley, S., Rosen, P. & Gurrola, F. 2000. Topographic map generation for the Shuttle Radar Topography Mission C-band SCANSAR interferometry. *Proceedings of SPIE **4152**, Microwave Remote Sensing of the Atmosphere and Environment II*, 179.189.

[36] Balmer, R. (1999). The SRTM Mission: A world-wide 30 m resolution DEM from SAR Interferometry in 11 days. *Photogrammetric week '99*, Heidelberg: Wichmann, 145-154.

[37] Smith, B. & Sandwell, D. (2003). Accuracy and resolution of Shuttle Radar Topography Mission data. *Geophysical Research Letters*, **30**, 1467-1470.

[38] Balzter, H., Luckman, A., Skinner, L., Rowland, C. & Dawson, T. (2007). Observations of forest stand top height and mean height from interferometric SAR and LIDAR over a conifer plantation at Thetford Forest, UK. *International Journal of Remote Sensing*, **28**(6), 1173 - 1197.

[39] Mercer, B., Zhang, Q., Denbina, M., Schwaebisch, M. & Cloude, S. (2009). DTM extraction beneath forest canopy at L-band from experimental single-pass airborne PolInSAR system. *PolInSAR 2009*, ESA, in press.

[40] Cloude, S.R. & Papathanassiou, K.P., (2003). Three-stage inversion process for polarimetric SAR interferometry, *IEE Proceedings - Radar Sonar Navigation*, **150**(3), 125-134.